

Experimental Investigation of Natural Convective Heat Transfer through Porous Media

Adil. A. Alwan

University of Babylon / College of Engineering / Mechanical Engineering Department

Mothanna. T. Mohammed

University of Al-Qasim Green/ College of Agriculture

mothannafa@yahoo.com , mothanna@agre.uoqasim.edu.iq

Esra'a. J. Mohammed

University of Babylon / College of Engineering / Mechanical Engineering Department

ABSTRACT

The unsteady natural convective heat transfer parameters through porous media sample were investigated experimentally. The sample consists of solid and fluid phases arranged as a matrix balls insulated from sides, and subjected to heat flux at the bottom surface as a boundary condition. The unsteady effects of associated heat transfer parameters (h , Nu_e , Nu_f and Ra_m) were calculated from the spatial and temporal distribution of temperature profile at different locations of sample measured by using temperature recorder device with SD memory card data logger with sensor type K thermocouple. It was found that these parameters were dependent upon the heating time, and the dimensions of solid and fluid layers of sample. In addition the pressure difference of air inside a void space has been measured by using the pressure reading device. Then, the fluid velocity and Reynolds number through heating process can be calculated. It was found that the values of air velocity are less than 0.08 m/s. The Reynolds number was experimentally less than 10.

KeyWords: Natural heat convection through porous media, Pressure measurement, Fluid velocity, Reynold number, Rayleigh number, Grashof number .

الخلاصة

في هذا البحث تدراسة معاملات انتقال الحرارة بالحمل الطبيعي خلال وسط مسامي عملياً. فقد تم افتراض أن العينة مكونة من طورين (صلب وسائل) مرتبة في مصفوفة من كرات معزولة من الجانبين وتم تسخينها من الاسفل كشرط حدي خارجي. بتأثير عدم الاتزان الحراري نتيجة التسخين، تم حساب معاملات انتقال الحرارة (h , Ra_m , Nu_f , Nu_e) للمادة المسامية من خلال قياس توزيع درجة الحرارة في مواقع مختلفة باستخدام جهاز تسجيل درجة الحرارة. فقد لوحظ اعتماد قيم هذه المعاملات على زيادة زمن التسخين والابعاد للطبقات الصلبة والسيولة للعينة. وبالإضافة إلى ذلك تم قياس فرق ضغط الهواء داخل الفراغ للوسط المسامي باستخدام جهاز قراءة الضغط. ومن ثم حساب سرعة السائل وعدد رينولدز خلال عملية التسخين. وتبين أن قيم سرعة الهواء أقل من 0.08 م / ث. وكان عدد رينولدز تجريبياً أقل من 10.

كلمات مفتاحية: الحمل الحراري الطبيعي، الوسط المسامي، مقياس الضغط، سرعة المائع، عدد رينولدز، عدد رايلي، عدد كراشوف.

1. INTRODUCTION

Due to the wide range of situations in which porous media are encountered, heat mechanism in these systems has received great deal of attention from both scientific and engineering communities. An understanding of heat transfer and fluid flow in porous media is important in many engineering fields, such as soil mechanics, powder metallurgy, chemical processing, petroleum reservoir, and high performance insulation for building and power collector.

Experimental studies dealt with the investigation of the steady free convection in a porous medium on natural convection in a horizontal porous layer heated uniformly from below. Glass spheres of diameter 3, 5, 8 and 18 mm and plastic balls styropor 6mm were used as the porous layer with distilled water as the saturating

fluid. It has been found that Ra_m around 40, there is an abrupt change in the value of the Nusselt number indicating that the onset of convection occurs when the Rayleigh number reaches the theoretically predicted critical value of $4\pi^2$. It has also been showed that the transferred heat across the layer is proportional to the square of the temperature difference across the layer and is independent of the thermal conductivity of the medium or the depth of the layer, reported by (Elder, 1967)

Bagchi (2010) observed that experimentally the natural convection in a horizontal fluid-superposed porous layer heated locally from below. He performed the experiments to validate the numerical solutions, and to develop empirical Nusselt versus Rayleigh number correlations. Experiments were conducted in a cubical chamber with 3 mm diameter glass beads as the porous layer and distilled water as the saturating fluid. Experimental results confirmed the numerical predictions that the Nusselt number increases with a decrease in the heater length and an increase in the height ratio. He also presented a comparison of the numerical and experimental results. The percentage of difference between the numerical and experimental data is $\geq 60\%$. He indicated that the numerical simulations agree with experimental results in the high Rayleigh number range of 4×10^7 .

The principle interest of this study was to identify the effect of dimensions of sample of measuring the overall heat transfer parameters inside the macrostructure of the sample which consisted of two phases arranged as a matrix balls to represent a porous media.

2. APPARATUS AND PROCEDURE

Experiments were carried out in cubic sample with dimensions (106.25 × 106.25 × 57.75) mm, filled with uniform Chrome–Steel balls of 17.25 mm diameter arranged as matrix of (5 × 5 × 3) particles. The lower plate of the sample is from iron of 3 mm thick, which was subjected to a uniform heat flux. While, the upper surface of the sample is from glass of thickness 3 mm. Number of thermocouples are fixed on the balls and inside the voids space at different position. They were arranged as six thermocouples fixed on the balls in each level, one in the center and the others in one corner. There are also four thermocouples distributed in the void between the balls, two in each level. The test sample of porous media was shown in Fig.1 and Fig.2. Number of holes is made at the upper surface to let the thermocouples throughout to the temperature recording device. There are two holes on the side surfaces for the horizontal pipes of the pressure reading device to read the pressure difference between the first void and the second void inside the sample. The heater was fixed at the bottom surface of the sample. Then, the sample is insulated from the sides by using a glass wool.

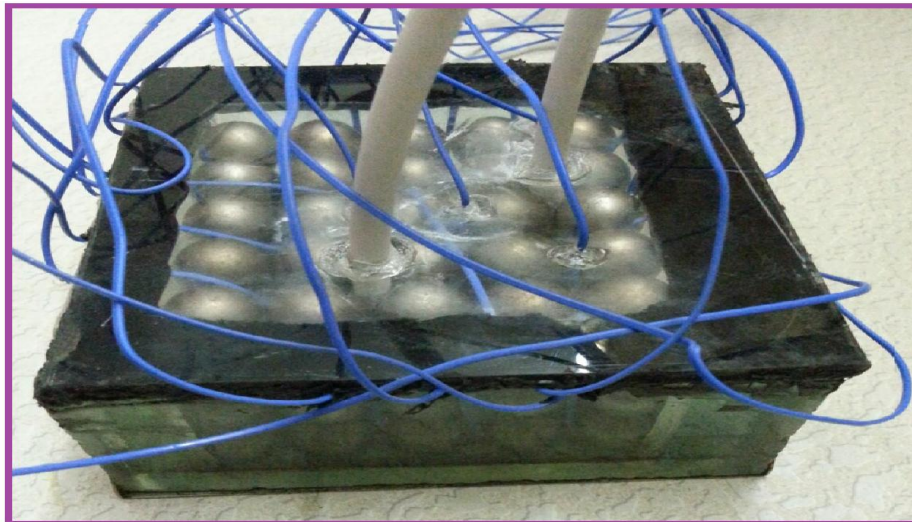


Fig.1. The photograph diagram of the sample

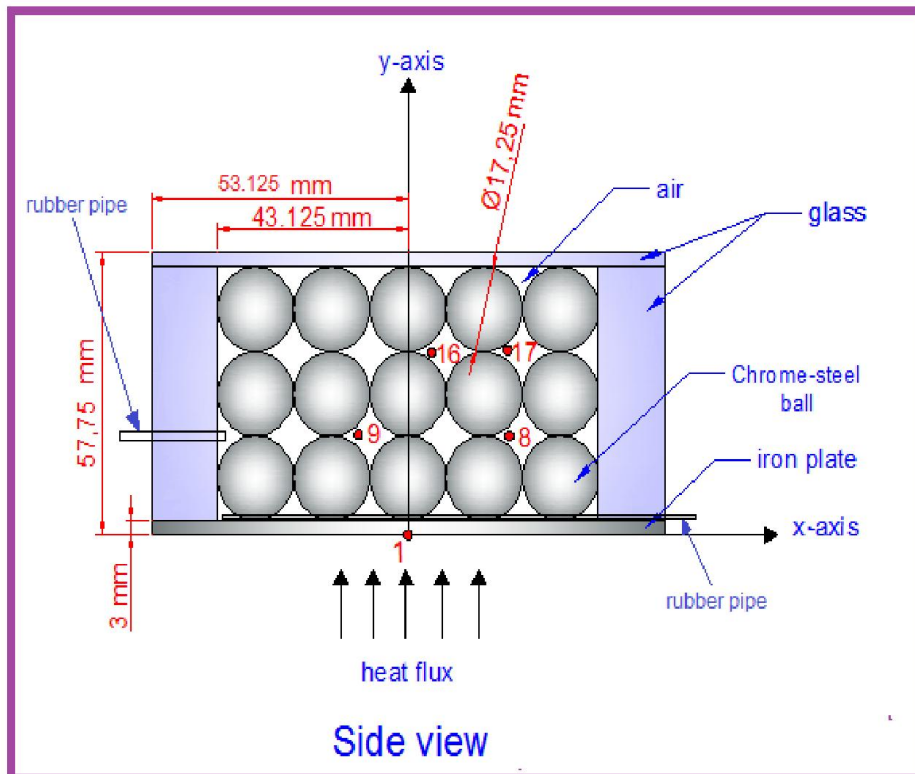


Fig.2. Schematic diagram for location of thermocouples on the sample

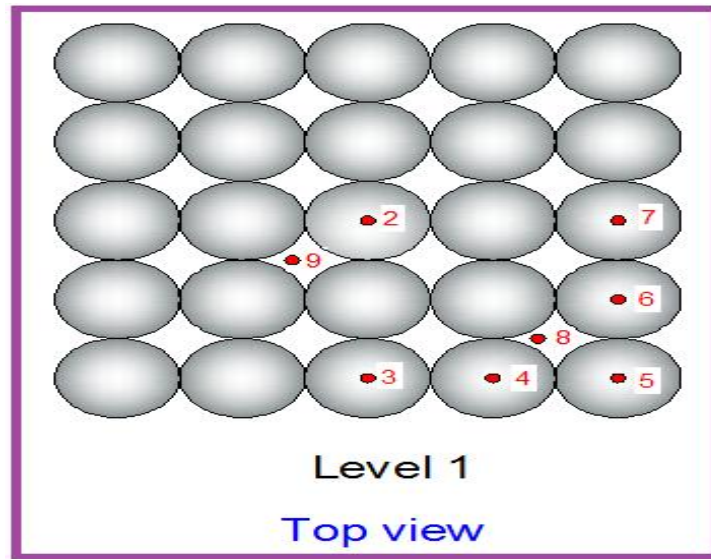


Fig.2. Schematic diagram for location of thermocouples on the sample

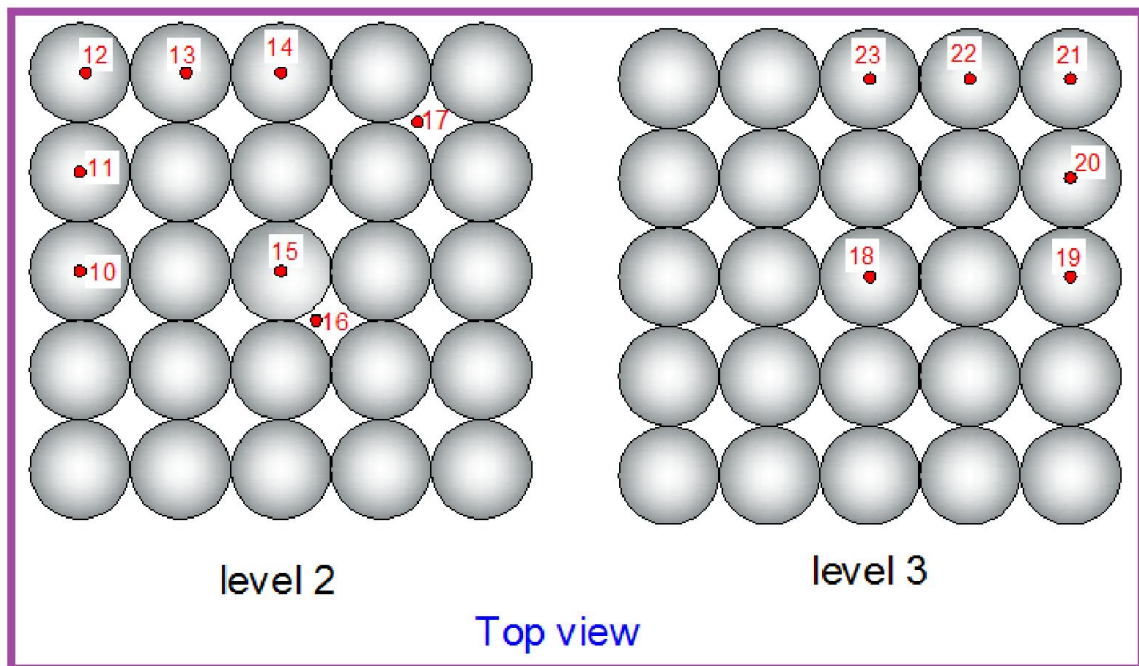


Fig .2.Schematic diagram for location of thermocouples on the sample

The schematic description of the experimental facility is presented in Fig.3.

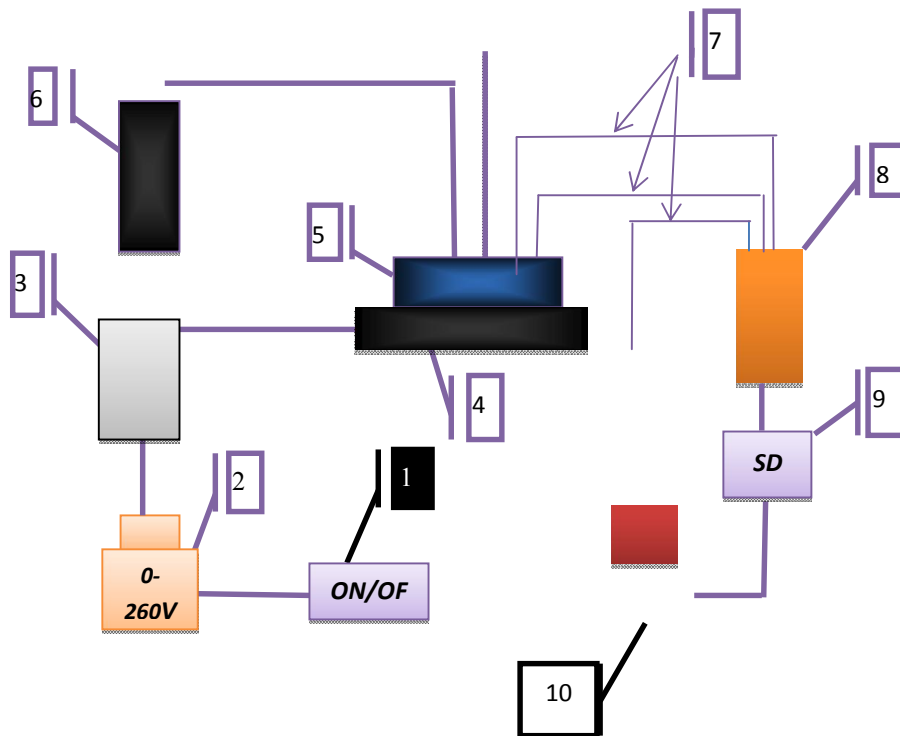


Fig.3. Experimental facility: (1) Power supply, (2) Voltage control device, (3) Power analyzer, (4) Heater, (5) Sample, (6) Micro manometer device, (7) Thermocouples, (8) Temperatures recording device, (9) SD Ram, (10) Computer.

Twenty three thermocouples type K (chromium-aluminum⁺) were fixed inside the macrostructure of sample at different locations to measure the two phase solid- air temperature. Temperature recorder with SD memory card data logger with sensor type K thermocouple was used to read the temperature with time. The digital readings of the temperature recording device has been calibrated with thermometer where the temperature was measured with varying temperature of porous media sample by using the temperature recording device for range temperature (0°C to 80°C), then it was compared with the reading of the thermometer as it is shown in figure (4-17). Relation between thermometer reading and that measured by temperature recorder was polynomial equation used to correct the temperature recorder reading.

$$T_{calib} = 1.21209 + 1.03027T_{re} - 0.0002078T_{re}^2 \dots\dots\dots (1)$$

Where T_{calib} is the calibrated temperature, T_{re} is the temperature of the temperature recorder measurement. This equation from thecalibration curve ofthe temperature recording device as it is shown in figure (4). The equation gave more reliable results and minimizes the errors through the measurement in order to get accurate results for the measurement of temperature distribution.

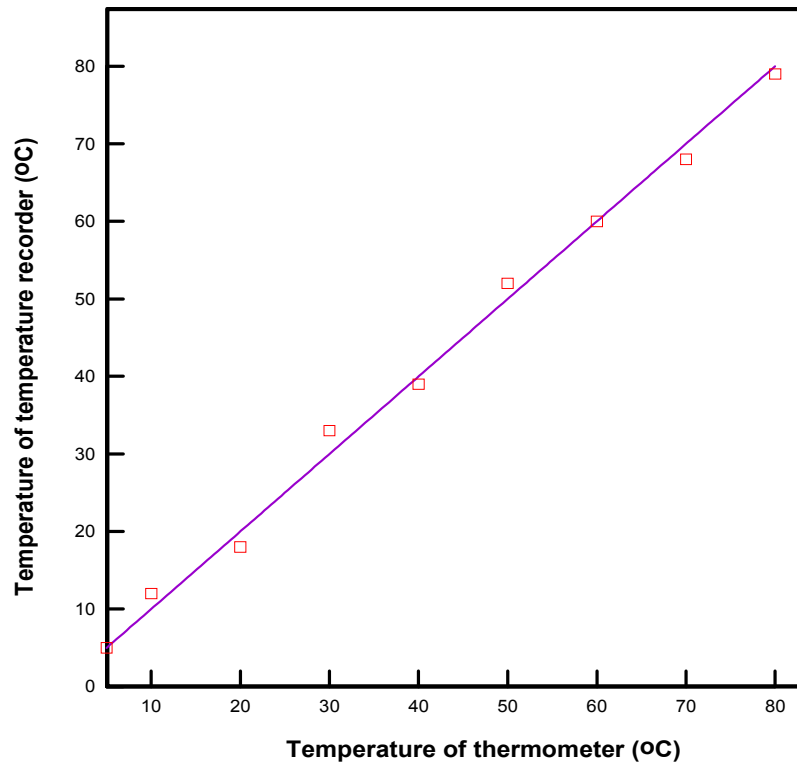


Fig. 4 calibration curve of the temperature recording device

A micro manometer model AXD530 was used to measure the air pressure inside the void space of the sample, with range pressure measurement (-250 to 2500) pa, and resolution 1 pa. This digital reading of the pressure reading device was by the company of this device. So, it has been gotten accurate results for the measurement of the pressure difference of the air inside the void space of the sample.

The voltage variation device turned on and started to control the voltage variation until it reached to the required value, then the power was supplied to start the heating process for the sample. The test was repeated at different values of the power supply.

3. ANALYTICAL CONSIDERATIONS:

The power was supplied to start the heating process for the sample. The electrical power supplied to heat the sample was calculated as reported by (The rajaetal, 2005).

$$P = V \times I \times 0.83 \quad \dots\dots\dots (2)$$

The heat transfer parameters (h , Nu_e , Nu_f and Ra_m) were calculated for local thermal equilibrium model by using the measured temperature $T_{t,s}$ and T_{bulk} after calibrated. The local heat transfer coefficient is defined by (Jiang and Lu, 2006) as:

$$q = hA\Delta T \quad \dots\dots\dots (3)$$

$$\frac{q}{A} = \text{heatflux} = q'' ,$$

$$\text{Then, } h = \frac{q''}{\Delta T} \quad \dots\dots\dots (4)$$

$$\text{Where } \Delta T = T_{t,s} - T_{bulk} \quad \dots\dots\dots (5)$$

When the focus upon natural convection alone, then the porous media would be modeled as a continuum having macroscopic properties ,including a stagnant effective

thermal conductivity. Hence the parameter of interest would then be a Nusselt number based upon the stagnant effective thermal conductivity, that is:

$$Nu_e = \frac{h.H}{k_e} \dots\dots\dots (6)$$

Then the value of Nu_f was calculated with the value of heat flux, which is given by (Holman, 2002) as:

$$Nu_f = \frac{hH}{k_f} \dots\dots\dots (7)$$

Where k_s and k_f are the thermal conductivity for solid and fluid phases. It can be easily to find the effective thermal conductivity for the sample as it is detailed by (Hans, 1999) as:

$$k_e = \phi k_f + (1 - \phi)k_s \dots\dots\dots (8)$$

Where ϕ is the porosity of the sample, which is defined by (Michele, 2010).

$$\phi = 1 - \frac{V_{solids}}{V_{total}} = \frac{V_{voids}}{V_{total}} \dots\dots\dots(9)$$

Where V_{solid} Volume of solid, V_{total} Total volume and V_{void} Volume of void .

(Nield and Bejan, 2006), they perform a linear stability analysis using the Darcy flow model to predict the onset of convection current. They considered that the onset of convection occurs when $Ra_m \geq 4\pi^2$. Where Ra_m is the porous media Rayleigh number, which is defined as:

$$Ra_m = \frac{K\rho_o g\beta H\Delta T}{\mu_f \alpha_e} \dots\dots\dots (10)$$

Then
$$\alpha_e = \frac{k_e}{(\rho c_p)_e} \dots\dots\dots (11)$$

Where α_e is the effective thermal diffusivity of porous media. The permeability of the porous media is also defined as a measure of the ability of a porous material to let fluids owing through it and it depends only on the geometry of the media not on the properties of the fluid. The size of the pores and their shape are the characteristics that influence the permeability value. (Combarous and Bouries, 1975) are using the Carman and Kozeny relationship that relates permeability and porosity, which it states as:

$$K = \frac{d^2}{172.8} \frac{\phi^3}{(1 - \phi)^2} \dots\dots\dots (12)$$

In which d is the diameter of the beads and the constant 172.8 was obtained by seeking the best of experimental results as pointed by (Tan and Sam, 1999).

It is important to experimentally calculate the velocity of the air inside the void space for the local thermal non-equilibrium model. This can be done by using the values of the measured pressure difference from the pressure reading device after calibrated. (Nabovati and Sousa, 2007) showed in this approach that air flow is simulated in the inter grain region and inside the pores of the porous media by using Darcy law over the domain, which has the form:

$$v = \frac{K}{\mu} \left(-\frac{dp}{dy} \right) \dots\dots\dots (13)$$

Where μ the dynamic viscosity of the fluid and K is the permeability of the porous media. In order to take into account the gravity field influence on the system at heating process from below, the term $\rho_o \cdot g$ is usually added to the momentum balance equations, then equation (13) becomes:

$$v = \frac{K}{\mu} \left(-\frac{dp}{dy} + \rho_o \cdot g \right) \dots\dots\dots (14)$$

Where g is the gravitational acceleration and ρ_o is the density at the temperature T_o . Darcy's law has been verified by the results of many experiments. Many authors have used statistical concepts to find a theoretical support for Darcy's law. This was done by using Darcy equation with the buoyancy term simplified by the Oberbeck-Boussinesq approximation. (Oberbeck,1879) and (Boussinesq,1903) assumed that all the physical properties of the fluid are independent on temperature, except for the density in the gravitational body force term of the momentum balance equation. So, the density is considered as a linear function of the temperature, basically a Taylor series expansion around the reference value ρ_o is truncated to the first order as detailed by (Michele, 2010), namely:

$$\rho = \rho_o (1 - \beta(T - T_o)) \dots\dots\dots (15)$$

Where β is the volume coefficient of expansion defined as:

$$\beta = -\frac{1}{\rho} \left(\frac{\partial \rho}{\partial T} \right)_p \dots\dots\dots (16)$$

Where T_o is the reference temperature. This reference temperature is chosen as a nontrivial task because of the sensitivity of the results to the value of T_o . For clear fluids a reference study has been done by (Barletta and Zanchini, 1999). The Darcy's law equation (14) with the Oberbeck-Boussinesq approximation as it is defined by (Michele, 2010):

$$v = \frac{K}{\mu} \left(-\frac{dp}{dy} + \rho_o \cdot g \cdot \beta(T - T_o) \right) \dots\dots\dots (17)$$

The permeability-based Reynolds number can also be calculated as:

$$Re_K = \frac{v \rho_o \sqrt{K}}{\mu_f} \dots\dots\dots (18)$$

The thermal properties for the air and chrome-steel are listed in table (1) as they are reported by Holman [8].

Table 1 thermal properties for air and theSubstances

Substance	ρ (kg/m ³)	C_P (kJ/kg.°C)	k (W/m.°C)	$T_{melting}$ (°C)	μ (kg/m.s)
air	1.1774	1005.7	0.02624	—	0.000018462
Chrome-steel 25%Cr,20%Ni	7865	0.46	12.8	1510	—

The results for the sample are listed in table (2).

Table 2experimental results for heat transfer parameters

Heat flux W/m ²	Time (sec)	ϕ porosity	Δp (N/m ²)	ν (m/s)	Re_K	h W/m ² .°C	Nu_f	Nu_e	Ra_m
1000	1800	0.477	0.733	3.672E-02	0.295	374.734	142.810	0.559	6.14
	3600	0.477	1.228	6.172E-02	0.496	319.990	121.947	0.477	1.232
2000	1800	0.477	0.980	4.927E-02	0.396	372.636	142.011	0.556	12.297
	3600	0.477	1.475	7.444E-02	0.599	315.482	120.229	0.470	2.524

4. RESULTS AND DISCUSSION

Figures (5), (6),(7) and (8) illustrate the temporal variation of temperature profiles in a number of thermocouples measurement for the sample, which were fixed at points 1 to 23 on the Chrome-steel balls at the two values of heat flux. It has been shown that the temperatures of these balls were increasing with the increasing the time of heating. It has also been indicated that the temperature values of the balls which are at the same raw are much close to each other. Knowing that the temperature at the corner is the highest one, then the temperature values are decreasing in postions away from the corner.It has also been shown the similar behavior of increasing the temperature values with time when increasing the values of heat flux increase.It has been pointed, as comparing with the previous figure, that the temperature values were less than those of the first raw. This is because the first raw is very close to the heater.

Figures (9) and (10) describe the spatial temperatures distribution through y-direction at time 3600 seconds for the sample at the two values of heat flux respectively. As it can be seen in the figures, the distribution of temperature dropped continuously along the y-direction, showing a curvilinear temperature distribution pattern. So, the temperature of point 1 (where x and y=0) is the highest one depending upon the value of heat flux and time of heating. This is due to the position ofthispoint at the bottom of the sample (near the heat source). Then, upon moving upward the heat resistant increases causing a reduction in the temperature values.It has also been shown when the amount of heat flux rises the values of spatial temperature increase at the same time of heating.

Figure (11) fixes the temporal variation of average heat transfer coefficient with time for the sample at heat flux 1000 W/m². The values of heat transfer coefficient have been calculated from the experimental results. The descending values of heat transfer coefficient with ascending the heating time. This behavior of dropping the values of heat transfer coefficient is related to the notion that was obvious that the value of temperature difference between the surface of solid layer and the bulk temperature of fluid layer $\Delta T = T_{b.S}(x) - T_{bulk}(x)$ is very small at the beginning of heating process, and begins to increase with time. Then, ΔT increases very slightlywith the increasing time of heating. This means that the values of surface

temperature and bulk temperature are being much close to each other with increasing time of heating.

Figure (12) shows the experimental temporal variation of the effective Nusselt number Nu_e for the sample at heat flux 1000 W/m^2 . The values of Nu_e have been calculated from the experimental results. It has been pointed that the effective Nusselt number is decreasing gradually with time. That was closing to the results of many authors such as (Karamallah *et al.*,2013). Figure (13)describes the temporal variation of Nusselt number of fluid Nu_f for the sample at heat flux 1000 W/m^2 . The figure resembles the results of figure (9), which were indicated the same relation and response of average heat transfer coefficient. This is because the Nusselt number of fluid Nu_f is proportional and dependent to the value of onset of the heat transfer coefficient and the thermal conductivity of fluid phase (air). So, it decreases as the time of heating increasing.

Figure (14) describes the experimental relations between the effective Nusselt number Nu_e and the Rayleigh number of porous media for the sample. It has been pointed that there is a continuous rise in Ra_m with the dropping values of Nu_e . Figure (15) reports the experimental temporal variation of pressure difference with time for the sample at the two values of heat flux. It has been pointed that the values of ΔP are rising gradually with the increasing time of heating time. The figure gives a good comparison by showing the effects of increasing the heat flux value on ΔP . Figure (16) fixes the variation of the calculated air velocity inside the fluid phase with time for the sample at the two values of heat flux. It has been shown that the air velocity was increasing as the time of heating increased. This is due to the increase values of pressure difference with time. In this figure, it has been pointed as rising the values heat flux to 2000 W/m^2 the values of velocity are going up. This is due to the increase values of temperature and ΔP with heating. Figures(17) and (18)construct the experimental variation of the calculated air velocity with pressure difference inside the fluid layer for the sample at the two values of heat flux respectively. It has been pointed that the air velocity was ascending in linear positive relation with the pressure difference through the heating process. This is because of the dependence of the value of air velocity on the pressure difference by applying the Darcy law.

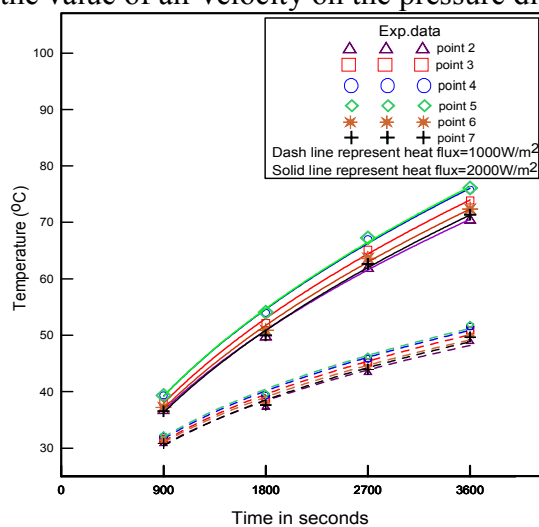


Fig.5. temporal variation of temperature at points (2,3,4,5,6 and 7)

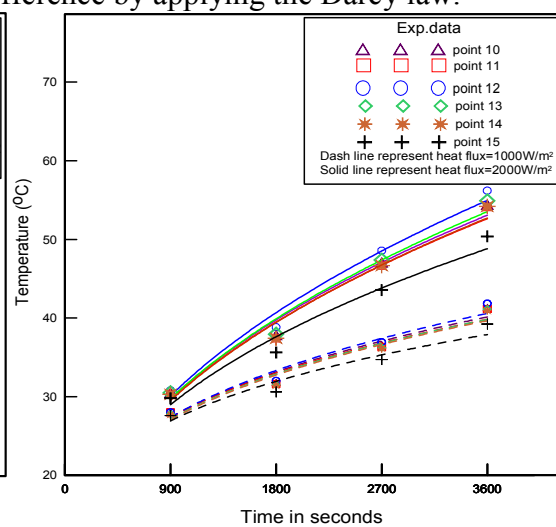


Fig .6.temporal variation of temperature at points (10,11,12,13,14 and 15)

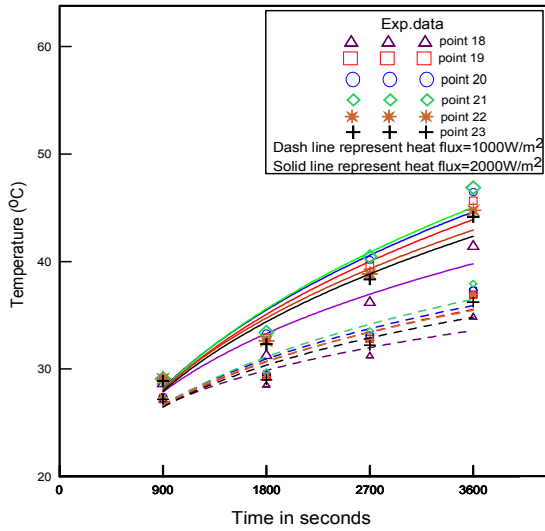


Fig. 7. temporal variation of temperature at points (18,19,20,21,22 and 23)

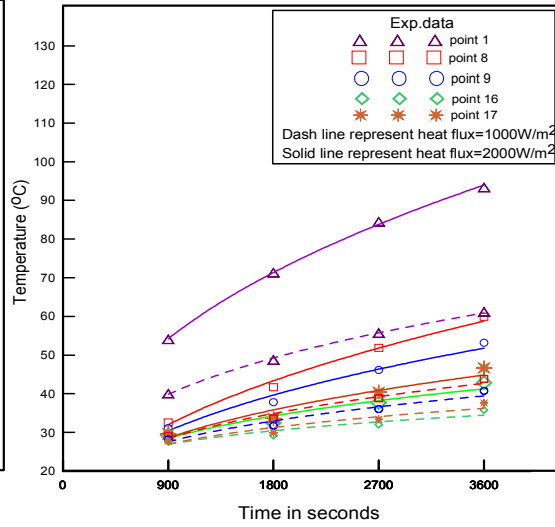


Fig. 8. temporal variation of temperature at points (1,8,9,16 and 17)

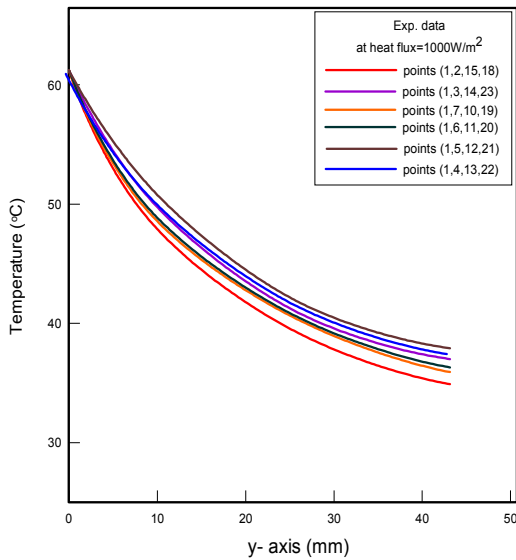


Fig. 9. spatial temperature through y-axis at 3600 seconds

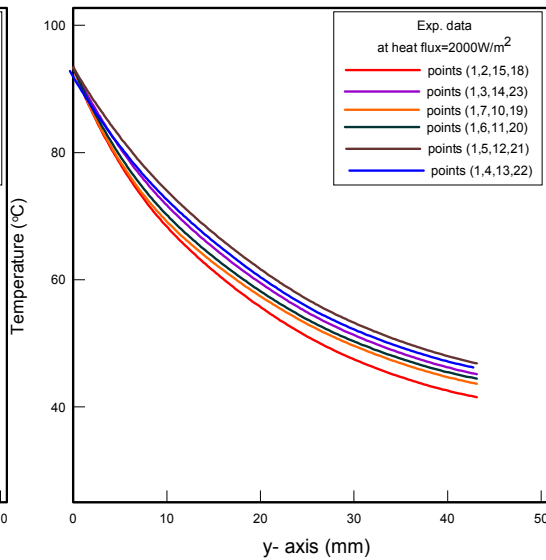


Fig. 10. spatial temperature through y-axis at 3600 seconds

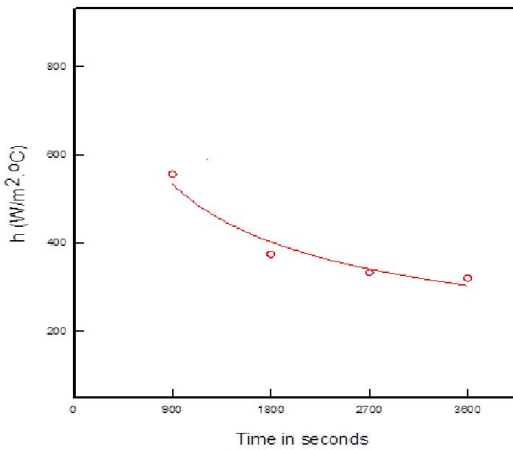


Fig. 11. temporal variation of average heat transfer coefficient at heat flux 1000 W/m²

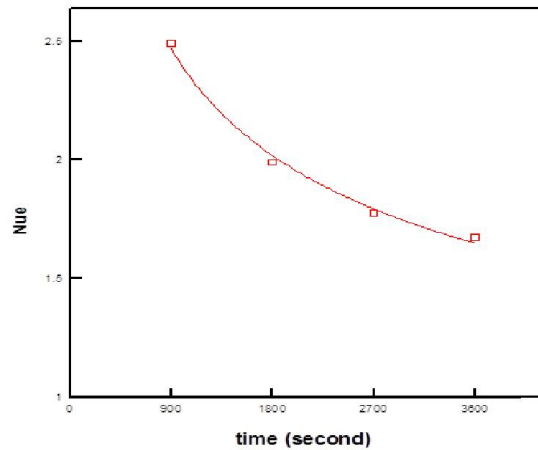


Fig. 12. temporal variation of effective Nusselt number at heat flux 1000 W/m²

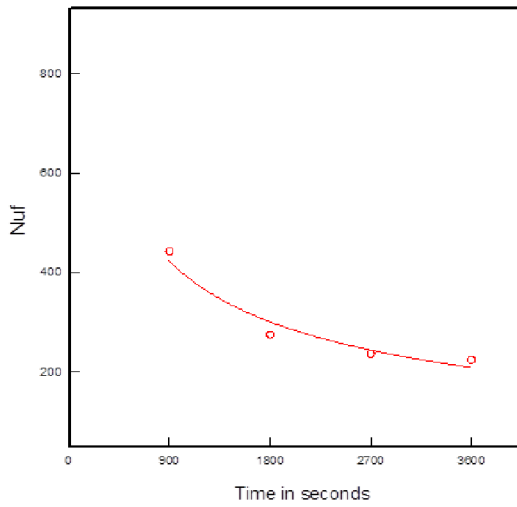


Fig .13. temporal variation of Nusselt number of fluid at heat flux 1000 W/m²

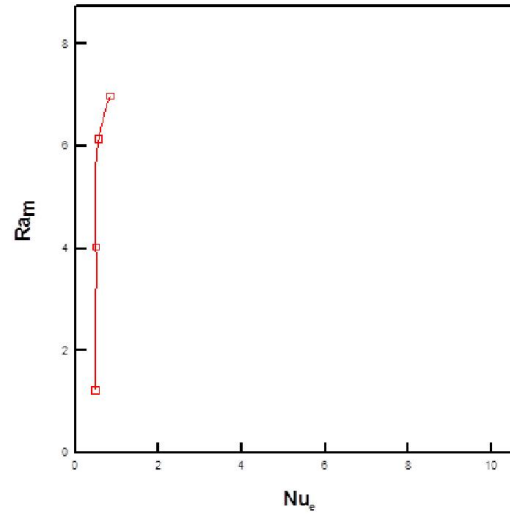


Fig .14. Nusselt number versus Rayleigh number at heat flux (2000 W/m²)

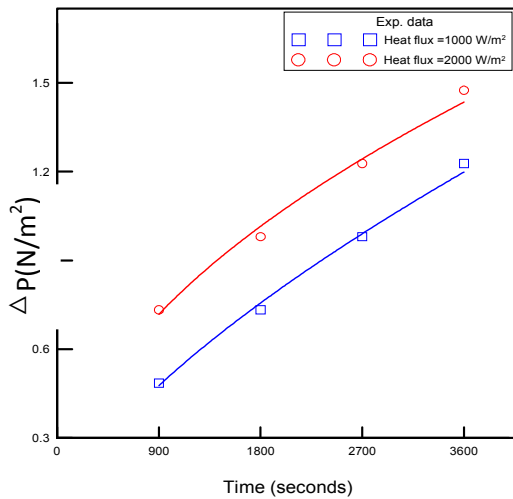


Fig .15. temporal variation of pressure difference

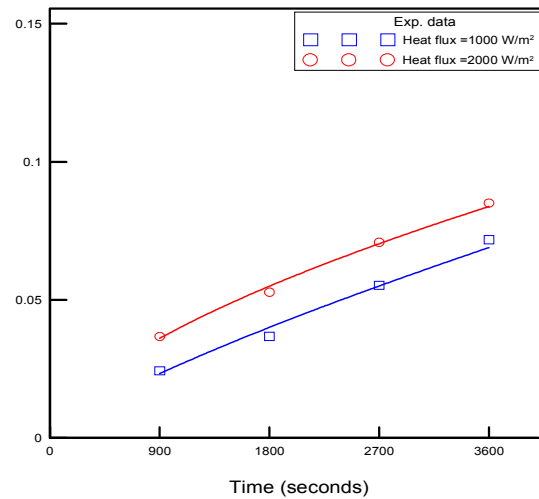


Fig .16. temporal variation of velocity

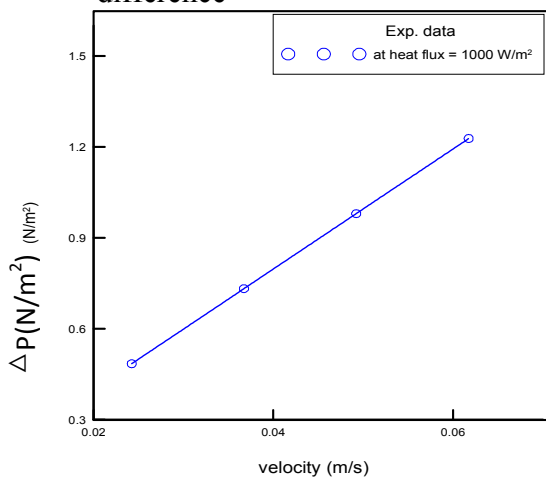


Fig .17. variation of pressure difference versus velocity

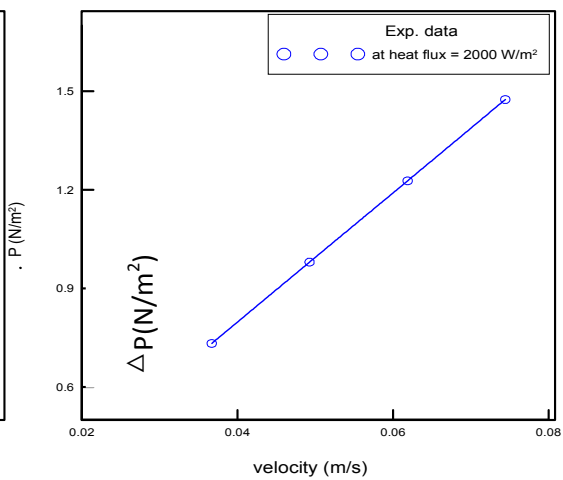


Fig .18. variation of pressure difference versus velocity

5. CONCLUSION

It has been found that the experimental measurements of temperature distribution through heating process agreed with perdition results of (Mohammed,2015).It has been shown that the heat transfer parameters (h , Nu_e and Nu_f) are decreasing with increasing the time of heating. It has also been pointed that the values of air velocity for the sample are less than 0.12 m/s, which are within the acceptable limit for the values of air velocity inside the porous media. Knowing that the values of Reynolds number for both works are less than 10 as it is confirmed by(Michele, 2010). It has also been yielded acceptable values of pressure difference inside the macrostructure of porous media.

NOMENCLATURE

C_p	Specific heat	J/kg. ⁰ C
d	Diameter of the bead	m
Da	Darcy number	---
g	Acceleration of gravity	m/s ²
h	Local convection heat transfer coefficient	(W/m ² . ⁰ C)
H	Layer thickness	m
I	Current	Ampere
k_e	Effective thermal conductivity	W/m. ⁰ C
k_f	Thermal conductivity of fluid	W/m. ⁰ C
k_s	Thermal conductivity of solid.....	W/m. ⁰ C
K	Permeability	m ²
L	Layer width	m
Nu_f	Nusselt number of fluid	---
Δp	Pressure difference	N/m ²
P	Power	W
Q	Heat	W
q''	Heat flux	W/m ²
Ra_f	Rayleigh number of fluid	---
Ra_m	Rayleigh number of porous media.....	---
Re	Reynolds number	---
t	Time	second
T_{bulk}	Bulk temperature	⁰ C
$T_{b.s}$	Temperature of the bottom surface	⁰ C
$T_{t.s}$	Temperature of the top surface	⁰ C
ΔT	Temperature difference	⁰ C
V	Velocity in y-direction	m/s
V_{solid}	Volume of solid.....	m ³
V_{total}	Total volume	m ³
V_{void}	Volume of void	m ³

V	Voltage	Volt
α_e	Effective thermal diffusivity	m^2/s
α_f	Thermal diffusivity of fluid	m^2/s
α_s	Thermal diffusivity of solid	m^2/s
β	Coefficient of volumetric expansion	$1/^\circ C$
ϕ	Porosity	---
μ	Dynamic viscosity	$kg/m.s$
ρ	Density	kg/m^3
$(\rho C)_e$	Effective heat capacity	$J/m^3 \cdot ^\circ C$
$(\rho C)_f$	Heat capacity of fluid	$J/m^3 \cdot ^\circ C$
$(\rho C)_s$	Heat capacity of solid	$J/m^3 \cdot ^\circ C$

REFERENCES

- Bagchi, A., 2010 "Natural Convection in Horizontal Fluid-Superposed Porous Layers Heated Locally From Below," Ph.D. Thesis, University of Minnesota.
- Barletta, A and Zanchini, E. , 1999, "On the Choice of the Reference Temperature for Fully Developed Mixed Convection in a Vertical Channel," Int. Journal of Heat and Mass Transfer, Vol. 42, pp. 3169-3181.
- Boussinesq, J., 1903 "Théorie Analytique de la Chaleur," Gauthier-Villars, Paris, Vol. 2.
- Combarnous, M. A., and Bories, S. A., 1975 "Hydrothermal Convection in Saturated Porous Media ," Adv. Hydroscience, Vol. 10, pp. 231–307.
- Elder, J. W., 1967 "The Unstable Interface ," Journal of Fluid Mech, Vol. 32, pp.69-69.
- Hameed, R., Alwan, A. and Ibraheem, E., 2012 "The Impact of the Fluid Layer Thickness on the Onset of Transient Convection in Porous Media," Journal of Babylon University, Vol. 20, No.7.
- Hans, T.A., 1999 "The Effective Thermal Conductivity of Saturated Porous Media," M.Sc. Thesis, University of Minnesota.
- Holman, J.P., 2002 "Heat Transfer," Book, Ninth Edition McGraw-Hill.
- Jiang, P.X., and Lu, X.C., 2006 "Numerical Simulation of Fluid Flow and Convection Heat Transfer in Sintered Porous Plate Channels," Int. Journal of Heat and Mass Transfer, Vol. 49, pp. 1685–1695.
- Karamallah , A.A., Hussain, I.Y., and Alwan, D.H., August 2013 " Experimental Study of Natural Convection Heat Transfer in Confined Porous Media Heated From Side," Journal of Engineering, Vol. 19, No. 8, pp. 952-969.
- Michele, C., 2010 "Stability, Viscous Dissipation and Local Thermal non-Equilibrium in Fluid Saturated Porous Media," Ph.D. Thesis, University of Bologna.
- Mohammed, E.J., 2015 "Unsteady Effects on Natural Convective Heat Transfer through Porous Media," M.Sc. Thesis, University of Babylon.
- Nabovati , A. , and Sousa , A. C. M., , 2007 " Fluid Flow Simulation in Random Porous Media at Pore Level Using the Lattice Boltzmann Method ," Journal of Engineering Science and Technology, Vol. 2, No. 3, pp. 226- 237.
- Nield, A.D., and Bejan, A., "Convection in Porous Media," Third Edition. Springer, New York, 2006.

- Oberbeck, A., 1979" Ueber die Wärmeleitung der Flüssigkeiten bei Berücksichtigung der Strömungen infolge von Temperatur - differenzen," Ann. Phys . Chem., Vol. 7, pp.271–292.
- Tan, K. K., and Sam, T., 6-8 December 1999 "Simulation of the Onset of Transient Convection in Porous Media under Fixed Surface Temperature Boundary Condition", 2nd International conference on CFD in the Minerals and Process Industries.
- Theraja, B.L., 2005Tarneker, S.G., Teraja, A.K., " A Text Book of Electrical Technology," Book , P.447 pages Published.